CONFERENCE PRE-PRINT

RUNAWAY ELECTRONS IN JET – SUMMARY ON RE DATA AFTER THE END OF JET OPERATIONS

V.V. PLYUSNIN

Instituto de Plasmas e Fusão Nuclear, Instituto Superior Técnico, Universidade de Lisboa,

Lisboa, Portugal

E-mail: vladislav.plyusnin@ipfn.ist.utl.pt

C. REUX, E. JOFFRIN

CEA, IRFM

Saint-Paul-les-Durance, France

V.G. KIPTILY, P. J. LOMAS, S. GERASIMOV, A. BOBOC

UKAEA, Culham Campus

Abingdon, United Kingdom

A.E. SHEVELEV

Ioffe Institute,

St. Petersburg, Russian Federation

A. HUBER

Institute of Fusion Energy and Nuclear Waste Management-Plasma Physics, Forschungszentrum Jülich GmbH, Jülich, Germany

O. FICKER, J. MLYNAR

Institute of Plasma Physics of the CAS

Prague, Czech Republic;

S. JACHMICH, M. LEHNEN

ITER International Organization,

 \S THE EUROFUSION TOKAMAK EXPLOITATION TEAM and * JET CONTRIBUTORS

Abstract

The Joint European Torus (JET) tokamak ended operations in December 2023. Main parameters of runaway electrons (REs) generated during major disruptions in JET have been numerically processed and compiled into summarizing data-base. Experimental data collection covers more than 2000 of runaway electron (RE) generation events observed during all stages of JET operations: during disruptions in JET with original plasma shape (JET-OPS, plasma cross-section is S_{plasma}≤ 7.8 m², with metal and carbon limiters); in a series of dedicated RE experiments after divertor installation inside the JET vacuum vessel (S_{plasma}≤ 4.7 m², plasma facing components (PFC) based on carbon fiber composite tiles (CFC) were used in JET-C till to 2009); and in JET with ITER-like Wall (JET-ILW experiments, from 2011). The manuscript presents an analysis of differences and similarities in phenomenology and comparison of the RE parameters measured in spontaneous disruptions, during those triggered by constant gas puff, Massive Gas Injection (MGI) and Shuttered Pellet Injection (SPI), including the latest experiments on benign RE termination. The data for RE generation analysis has been retrieved manually using JET Logging System and Session Report generator, and combined with some early JET results on RE studies. RE beam macroscopic parameters were consolidated with the data on HXR/γ and photo-neutron radiations for evaluation of RE energy in different JET disruption scenarios. Performed analysis of CQ characteristics allowed establish trend in dynamics of RE parameters enabling their extrapolation to scale of ITER operation parameters.

1. INTRODUCTION AND STATISTICAL SUMMARY ON RUNAWAY ELECTRONS IN JET

Main efforts of nuclear fusion research are focused on the mastering of complex technology of a fusion reactor, which will enable the generation, heating and confinement of plasmas in the "burning regime". It should result in a creation of the energy source, based on use of energy of controlled fusion reactions for electricity generation and, simultaneously, allowing to sustain the plasma hot enough requiring no external energy for heating. Recent experiments have demonstrated that one of the most advanced types of such devices for controlled fusion is a tokamak. International Thermonuclear Experimental Reactor (ITER) being currently under construction in Cadarache in southern France is based on the tokamak concept [1-3]. Operating near equilibrium and stability boundaries tokamak plasma discharges very often could achieve conditions of emergency termination, which is called major disruption [4]. Plasma major disruptions pose severe threats to the device integrity in future operations of ITER. Major disruptions can cause excessive electromagnetic forces, heat loads onto plasma facing

Deceased

[§]Author's list of "Overview of the EUROfusion Tokamak Exploitation programme in support of ITER and DEMO" by E. Joffrin et al 2024 Nuclear Fusion 64 112019

^{*}Author's list of "Overview of T and D-T results in JET with ITER-like wall" by C.F. Maggi et al 2024 Nuclear Fusion 64 112012;

components (PFC), and an induction of strong electric fields occurring during plasma energy collapse and plasma current decay, i.e., during thermal and current quenches (TQ and CQ). If these electric fields are strong enough to overcome the dissipative effect of the Coulomb collisions, they accelerate plasma electrons into runaway regime [5]. Such runaway electrons (REs) will be accelerated ever more rapidly because the collisional dissipation decreases with increase of electron velocity. Unlimited acceleration inevitably leads to the relativistic energies acquired by REs [6]. Major disruptions and REs have been investigated in many tokamaks. Experiments in JET [7-9], JT-60U [10], EAST [11], TORE Supra [12], DIII-D [13], in other devices [14] allowed documenting the conditions for generation of RE beams with energies up to several tens of Mega-electron-Volts (MeV) and densities high enough to create current plateaus up to 60-70% of the pre-disruptive plasma currents. Extrapolation calculated for ITER operation parameters [15] have demonstrated that during ITER disruptions one can expect the generation of RE beams with more than one half of pre-disruption plasma current (Ipi≤15 MA) in multi-MeV energy ranges due to avalanching amplification of seed RE populations [16,17]. Localized interaction of such intense RE beams with surrounding PFC in tokamak-reactor inevitably will lead to high thermal loads, sputtering and melting of PFC resulting in inacceptable device damage [18]. To avoid/suppress RE generation and mitigate other detrimental consequences of disruptions, the special system – Disruption Mitigation System (DMS) [19] – is under construction at ITER. This system is based on collisional (radiation) dissipation of the plasma energy released during disruptions and the dissipation of possible REs generated following the fast plasma shutdown [20]. Shattered Pellet Injection (SPI) is the baseline DMS method for both thermal and electromagnetic load mitigation (EL/TLM) and RE suppression [21-23]. A significant progress in studies relevant to the ITER DMS design and corresponding R&D work was achieved recently [23-25]. However, the set of physical and technology problems remains un-resolved. In particular, they concern to understanding of the physics of RE formation during fast injections of plasma fuel (Hydrogen/Deuterium/Tritium) and different impurities (frozen Argon, Neon, etc.). The mechanisms responsible for mixing and assimilation of injected materials in Shuttered Pellet Injection (SPI) are under intense studies [26]. Interaction of REs with injected materials during the rapid shutdown and with residual surrounding plasmas is the key problem in theoretical and experimental studies of runaway beam dissipation [23,24,26,27]. Reliable beam avoidance or dissipation requires a proper knowledge of conditions for runaway beams formation occurring during TQ and CQ stages in tokamak disruptions. Experiments in JET provided large amount of data on disruption dynamics and RE generation parameters allowing their extrapolation to scale of ITER operation parameters [26].

TABLE 1. A survey of JET operation stages and number of RE generation events detected during each period

Operational phases & plasma configurations, PFC materials and divertor configurations	Period	Last shot number	Detected RE generation events
materials and divertor configurations		Hullioei	generation events
JET- Original Plasma Shape (JET-OPS)	Operations till to August 1987	#12106	≈ 320 events
JET-OPS, Limiter, X-Point (SN, DN)	August 1987 - February 1992	#28791	≈ 560 events
JET-C – Divertor MKI + CFC tiles	March 1994 - June 1995	#35778	≈ 130 events
JET-C – Divertor MKIIA, AP + CFC tiles	May 1996 – Feb 1998 – Sept 1998	#45155	≈ 220 events
JET-C – Divertor MKIIGB +CFC tiles	July 1998 - March 2001	#54549	≈ 250 events
JET-C – Divertor MKIIGB SR + CFC tiles	Jul 01 - Mar 04; Aug 05 - Apr 07	#63445	≈ 150 events
JET-C – Divertor MKII HD + CFC tiles	Carbon wall ends 23-Oct-2009	#79853	≈ 150 events
JET with ITER Like Wall (ILW) + Divertor	ILW Experiments – from July 2011	#105929	\geq 340 events

Experimental data-base on REs contains a collection of plasma, disruption and RE parameters measured in more than 2000 runaway generation events registered during different periods of JET operations. Table 1 presents a statistical information on JET runaway generation events which have occurred over all JET operation stages. Plasma and disruption parameters documented in experiments till to the end of JET operations in December of 2023 have been retrieved manually from the main JET data storage system using the JET Logging system and Session Report generator. The data has been numerically processed, combined with revisited some early results of RE studies in JET, e.g., [7, 8, etc.] and compiled into comprehensive data-base on REs generated in JET. From the beginning of JET operations there were several limited attempts to review the data on RE generation during JET disruptions [7, 8, 28]. This paper presents extended survey of recent massive updates of RE data-base, which was developed at JET, thus providing substantial enhancement in understanding of physics of REs and contributing new data in the model developed for runaway electrons generated in tokamak disruptions.

2. INSTRUMENTATION FOR MEASUREMENTS OF RUNAWAY ELECTRON PARAMETERS

Disruption generated REs in JET have been diagnosed since the early operations (JET-OPS) [4, 28, 29]. Usually, RE generation event is associated with formation of the long persisting plasma current tails on CQ stage and simultaneous detection of intense bursts of HXR/γ 's and photo-neutron radiation. Observation of intense bursts

of HXR/γ 's and photo-neutron radiation on TQ and CQ (even without current plateau formation) indicates about the process of plasma electron acceleration till to relativistic velocities. Commonly, relativistic RE interacting with surrounding PFC, background plasma or neutrals produce a bremsstrahlung hard X-ray emission (HXR) in the MeV energy range and photo-neutron emission. To enable the photo-neutron reactions the HXR energy should be higher than the neutron bound energy of the target nuclei ε_n , which is for different material is: for deuterium – 2.2 MeV, beryllium – 1.7 MeV, carbon – 18.7 MeV, argon – 9.9 MeV, nickel – 12.0 MeV, copper – 10.6 MeV, tungsten – 7.4 MeV. The energy of produced photo-neutrons is $E_n = E_{HXR} - \varepsilon_n$. Extended set of JET diagnostics has been used to measure these radiations and to determine the parameters of RE and their temporal and spatial evolution [29, 30]. For the machine protection and RE studies 5 scintillation time-resolved HXR monitors and neutron rate fission chamber monitors (235U and 238U) at 3 different locations operate in a current mode with 0.1 ms time resolution. The HXR emission has been measured with the set of horizontally and vertically viewing NaI(Tl), Bi₄GeO₁₂ (mentioned as BGO) and LaBr₃ spectrometers. The data on spatial distribution of HXR emission sources in the plasma has been obtained with the JET neutron/gamma profile monitor routinely used for neutron and gamma-ray measurements. This monitor comprises two cameras, vertical and horizontal, with 9 and 10 lines of sight, respectively. Each camera has two detectors: NE213 - for neutron and HXR measurements, and CsI detector for HXR registration. The data from vertical and horizontal sets of the detectors enabled the tomography reconstruction of the runaway beam image in HXR. Numerical analysis of the measured HXR spectra provided the data on maximal energy of runaway electrons and allowed reconstructing the energy distribution of fast electrons in visible volume. As well, the soft X-ray (SXR) diagnostics consisting of vertical and horizontal cameras has been used to study the RE beams spatial evolution by the tomography reconstruction. Existing on JET the Fast Ion Loss Detector (FILD) allowed registering of high energy REs when disruption-born particles and radiations interacted with FILD scintillator and generated image in CCD camera.

3. DISRUPTION SCENARIOS FOR RUNAWAY ELECTRON STUDIES IN JET EXPERIMENTS

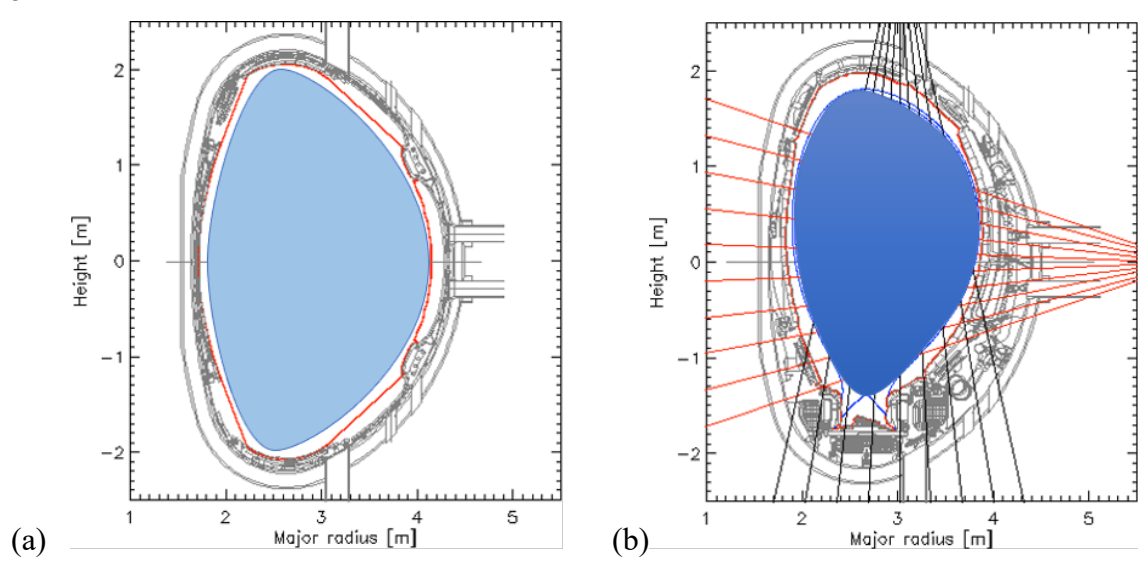


FIG. 1. JET plasma cross-sections: chart (a) – plasma cross-section and shape of the JET original design (Original Plasma Shape, JET-OPS, plasma area $S_{plasma} \le 7.8 \text{ m}^2$); chart (b) – JET plasma shape and area ($S_{plasma} \le 4.7 \text{ m}^2$) formed after the divertor coils installed inside the vacuum vessel (dark blue). Operations in JET with divertor & CFC tiles (JET-C) and operations in JET with metal ITER Like Wall (JET-ILW). Red and black lines drawn in chart (b) show the trajectories of JET neutron/gamma profile monitor lines of sight.

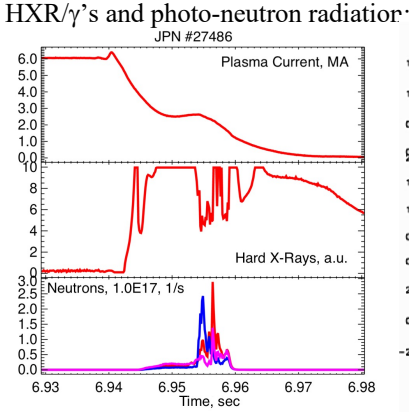
From the operational aspects several disruption scenarios provided the data on REs:

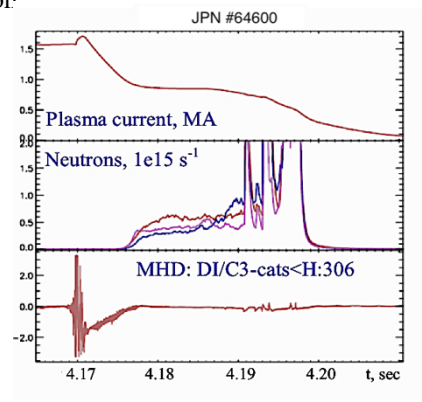
- scenario (a) spontaneous disruptions in JET with plasma shape of original design and cross-section area up to S_{plasma}≤ 7.8 m² (operations in JET with Original Plasma Shape JET-OPS). Cross-section of JET-OPS plasma is depicted in FIG. 1 (chart (a)). Inconel, carbon and beryllium (Be) have been used as limiter materials in JET-OPS experiments;
- scenario (b) series of dedicated RE experiments with disruptions triggered using slow gas puff (Ar, Ne, He) and MGI of Ar, Ne and their mixtures with working gas from the first DMV-1, as well as studies of REs in spontaneous disruptions have been carried out in JET after the installation of the divertor coils inside the vacuum vessel. The installation resulted in significant decrease of plasma cross-section area (S_{plasma}≤ 4.7 m², chart (b) in FIG. 1, dark blue). Carbon fiber composite tiles (CFC tiles) have been used in elements of PFC (operation period JET-C, till to 2009);

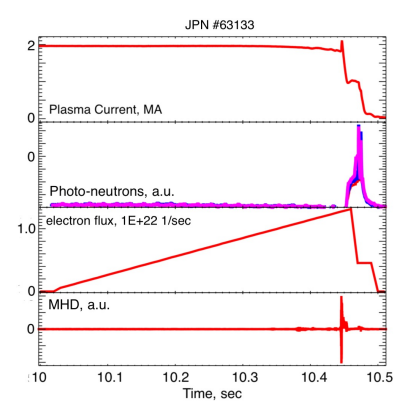
- scenario (c) - dedicated RE experiments in disruptions triggered by MGI (from three different DMVs) and SPI in JET after installation of ITER-like Wall (JET-ILW) with tungsten divertor and limiters made from beryllium (JET operations from 2011).

Several types of events depending on disruption phenomenology, CQ dynamics and detection of RE generation process have been categorized:

- 1) RE populations formed characteristic current plateaus during CQ (i.e., dIpl/dt=0, Ipl=Ires+IRE=const, Ires plasma resistive current, $I_{RE} - RE$ current fraction), with simultaneous detection of intense bursts of HXR/γ 's and photoneutron radiation. Sometimes after disruptions RE plateaus were lasting up to several seconds with runaway current fraction achieved 100% of the plateau;
- 2) RE population formed semi-plateaus (dI_{pl}/dt < 0) during CQ with obvious deviation of CQ evolution from exponential decay and relatively small runaway current fraction, with simultaneous detection of intense bursts of





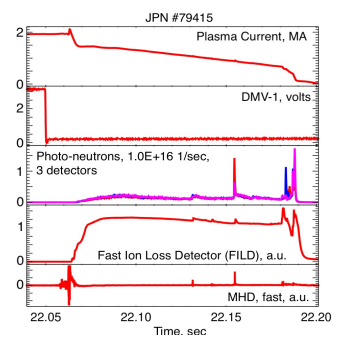


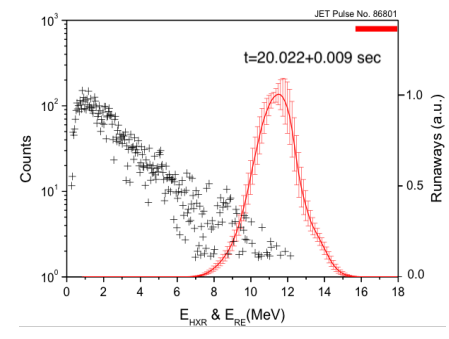
shown. RE current fraction is $I_{RE} \le 1.5$ presented.

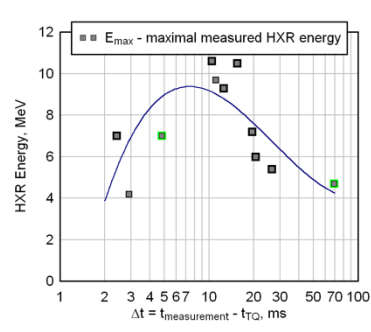
FIG. 2. High current JET-OPS FIG. 3. Spontaneous disruption in JET-C FIG. 4. RE generation in triggered by disruption ($I_{pl} \approx 6$. MA) with with RE generation. $I_{plateau} \leq 0.8$ MA and RE slow Ne puff disruption in JET-C. Time formation of RE plateau ($I_{plateau} \le 2.62$ current fraction is $I_{RE} \le 0.65$ MA. Temporal traces of plasma current, photo-neutron MA). Time traces of plasma current, evolutions of plasma current, photo-neutron emissions, equivalent electron flux and hard X-ray, photo-neutron signals are emission and fast MHD activity signals are MHD activity signals are shown.

Runaway current fraction is $I_{RE} \leq 1.2$

- 3) Scenario, in which intense bursts of HXR/y's and photo-neutron radiation on TQ and CQ have been detected (energies are high similarly to types 1) and 2), but measurable RE current fractions have not been detected;
- 4) Detection of the SXR and HXR/ γ 's bursts signified generation of REs with relatively low energies ($\leq 1 \text{ MeV}$).







current fraction is $I_{RE} \le 1.25 \text{ MA}$

FIG. 5. Disruption in JET-C FIG 6: HXR spectrum recorded with NaI(Tl) FIG. 7. RE energy evolution in JET. triggered by MGI with formation of detector (raw data, black crosses) from RE Hard X-Ray spectrometry in JET-C RE plateau. Temporal evolutions of population generated in disruption of disruption scenarios. NaI(Tl) detector, plasma current, FILD signal, discharge #86801 triggered in JET-ILW fast DAQ, integrated signal from vertical photo-neutrons and DMV trigger scenario with MGI, and energy spectrum of Line-of-Sight. Maximal RE energy E_{MAX} and MHD, I_{plateau} ≤1.45 MA RE REs reconstructed using de-convolution vs. time from the beginning of CQ procedure (red)[32].

CQ studies allowed distinguishing several groups of disruption dynamics resulting in RE process: with constant quench rates during in the beginning of decay, which corresponds to exponential decay of the resistive plasma current and very often followed by RE generation; the disruptions with substantially varied CQ rates with sometimes observed REs; and, a third group includes disruptions with RE but without measurable CO stage, i.e., when generation was detected immediately after the thermal quench with measurable SXR and HXR/y's and photo-neutron emission.

Figs. 2-5 present examples of runaway generation events and evolutions of key plasma parameters, which are commonly measured during JET disruptions. FIG.2 demonstrates evolution of plasma parameters in spontaneous disruption with $I_{pl} \approx 6.1$ MA (JPN #27486) occurred in JET-OPS experiments (scenario (a)): characteristic RE current plateau has been formed during CQ stage and subsequent intense bursts of photo-neutron radiation have measured by disruption monitors (235U and 238U fission chambers). The JET-OPS plasmas have been characterized by *d*-shaped plasmas (major radius $R_0 \le 3.0$ m, minor radius $a_{pl} = 1.25$ m and plasma elongation up to $b_{pl}/a_{pl} \le 1.7$) providing maximal plasma cross-section area up to S_{plasma} < 7.8 m², large stored plasma and poloidal magnetic field energies [31]. The JET-OPS experimental scenarios with plasma currents up to I_{pl}≤7 MA attracted a special attention because of such operation scenarios on plasma current and magnetic field values are close to one of the future planed ITER operation scenarios (7.5 MA/2.65 T). That is why RE generation during disruptions in this scenario has been documented and analyzed for understanding the trend in parameters of RE process toward the high disrupted plasma currents. In JET-OPS scenarios REs have been detected in several disruptions with currents $6.0 \text{ MA} \le I_{\text{pl}} \le 6.2 \text{ MA}$ and maximal plasma current achieved in disruption with $I_{\text{pl}} = 6.6 \text{ MA}$. Comparison of the influence of different PFC materials on RE process in JET-OPS has demonstrated that the probability of RE generation in disruptions with beryllium limiters was significantly lower than to those occurred in carbon-bounded (carbon-made PFC) and Inconel cases. Substantial decrease of plasma cross-section area to $S_{plasma} \le 4.7 \text{ m}^2$ led to corresponding limitation of the maximal plasma currents in JET-C and in JET-ILW experiments (Ipl \(\) 4.5 MA). Scenario (b) (FIG.3) enabled documenting of RE parameters measured in spontaneous disruptions and in disruptions triggered intentionally using the slow gas puff (FIG.4). Despite of significant differences in plasma geometry (divertor and limiter configurations, etc.) and physical operation parameters a majority of spontaneous disruptions occurred in JET-OPS and JET-C revealed very similar phenomenology and RE generation dynamics. Measured parameters of REs were included into data-base. MGI system developed during JET-C operations has been used for studies of runaway generation and conditions for REs avoidance/suppression (FIG.5). Unlike slow gas puff, the MGI scenario resulted in fast penetration (~500 m/s) of the cooling front into plasma core up to the critical radius of flux surface, triggering fast energy collapse. Up to 2.5E+23 particles could be injected during MGI at a maximum pressure in DMV gas storage chamber. In analyzed experiments amount of injected argon or neon (or their mixtures with deuterium) has been varied between 4E+22 and 2.4E+23 atoms. Usually, the disruption occurred after MGI in 7 ÷ 10 msec, while the scenario with constant gas puff required significantly longer time (up to 0.5 sec) to trigger the disruptions.

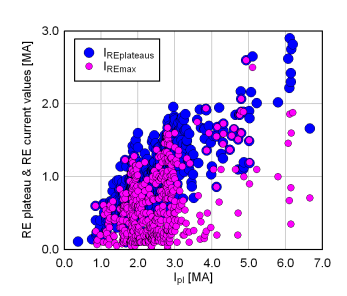
Massive injection (fast) of argon enabled RE generation with current values often larger that 1 MA and duration over 0.15 sec for all gas amounts used in JET-C (FIG. 5). Injection of neon resulted in much weaker runaway generation and no REs has been detected in disruptions triggered by MGI with mixtures of Ar/Ne with deuterium [9,20]. All disruption scenarios, in which plasma shut-down was caused by slow gas puff or fast MGI/SPI methods are based on the physics of density limit disruptions [4]. Note, that density limit scenario was found more suitable for RE studies during disruptions in conditions of limiter discharges. Following the strategy developed in JET-C experiments [20], MGI has been applied in JET-ILW experiments for mitigation of unwanted spontaneous disruptions [9]. Spontaneous disruptions in JET-ILW have shown substantial decrease of RE generation probability due to higher electron temperature detected immediately before and during the CQ, i.e., carbon or metal releases caused much stronger cooling effect in comparison to Be limiters [9]. Plasma current time derivative in the experiments was substantially lower thus limiting accelerating action of electric fields. Similar effect was observed in JET-OPS experiments when beryllium limiters were used [28]. Runaway beam formation has been studied in JET-C and JET-ILW MGI experiments [9,20]. These experiments has been carried out in circular and elongated plasmas establishing main conditions on generation and subsequent avoidance /suppression of REs [9,20]. On the basis of JET-C and JET-ILW MGI experiments the more efficient SPI scenario was developed enabling the formulation of conditions for benign termination of RE beams [24].

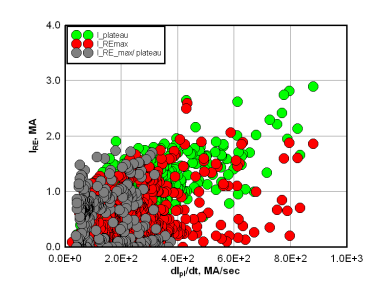
Measurements of HXR/ γ and photo-neutrons provided the information on energy characteristics of REs. The HXR emission has been measured with the set of different spectrometers (NaI(Tl), Bi₄GeO₁₂ and LaBr₃). The data on spatial distribution of HXR emission sources during disruptions has been obtained with the aid of JET neutron/gamma profile monitor routinely used for neutron and γ -rays measurements. The HXR raw data measured by spectrometers has been processed using de-convolution procedure (in detail see [32]). This procedure allows reconstruction of the energy spectra of generated RE populations (FIG.6).

Time-resolved measurements of the HXR spectra during CQs and plateaus in JET-C have revealed non-trivial time-depending evolution of RE generation process (FIG. 7). In this figure the maximal RE energies are plotted versus the time after beginning of CQ. Measurements of HXR spectra have been carried out in chosen time points during the CQ and plateau stages. To reduce the errors, the data was integrated over a time-interval of several msec. In order to interpret the evolution of the RE energy versus time the following sequence of processes should be considered. REs have been accelerated from the time close to beginning of CQ when plasma current time derivative is highest. RE energies achieved maximal values around 10-15 msec during CQ and revealed trend to decrease. In this time assessed RE current fractions in total plasma current begin to exceed the ohmic current thus

limiting and further diminishing electric fields and electron acceleration. The measured energies ($E_{MAX} \le 10 \div 12$ MeV) are too low in comparison to values expected from: $\gamma = \sqrt{1 + \left(\left(\frac{e}{m_e c} \cdot \int E_{\parallel 0}(t)dt\right)^2\right)} \sim 50 \div 60$ (for electric field $\sim 50 \text{ V/m}$, which is acting during 0.002-0.004 sec). Observed controversy requires an additional analysis described dynamics including numerical data processing and modelling.

MAIN TRENDS IN RUNAWAY ELECTRON PARAMETERS MEASRED IN ALL SCENARIOS OF MAJOR DISRUPTIOS IN JET





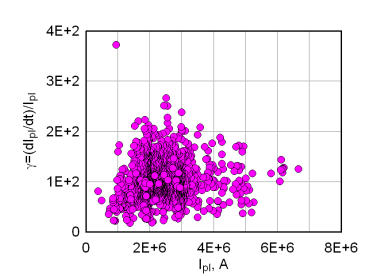
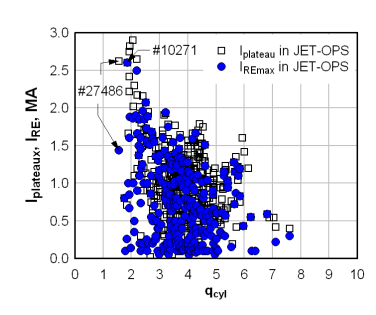


FIG 8. General trend in values of RE plateaus and inferred RE current fractions generated in all plasma disruption scenarios in a whole range of all plasma disruption scenarios disrupted currents

current plateaus and RE currents vs. $\gamma = 1/I_p * dI_p / dt$ vs. I_{pl} in whole range of plasma current time derrivative dI_p/dt in disrupted plasma currents resulted in

FIG.9. Dependence of generated RE FIG 10. CQ rate studies: CQ rate RE generation and mesured in all JET disruption scenarios.

Shot-by-shot analysis of disruptions in JET-OPS scenarios revealed the generation of runaway current plateaus up to 2.9 MA and maximal runaway currents IRE max up to 2.6 MA in disrupted discharges with high plasma currents ranging from 5 MA to 6.6 MA. Experiments in JET-C and JET-ILW provided the data on REs generated



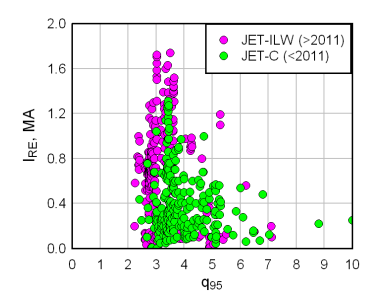
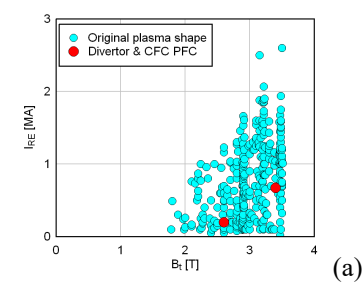
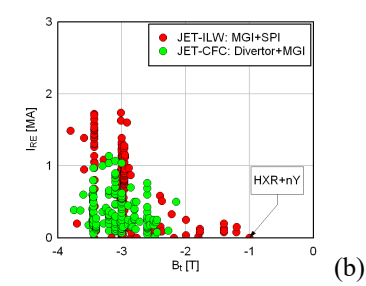


FIG.11. JET-OPS disruption data on FIG.12. Data on RE currents plateaus and generated in JET-C and JET-ILW calculated runaway current fractions disruption scenarios plotted vs. q95 RE studies and their interpretations plotted vs. q(a)(EFIT data)

in disruptions with plasma currents up to 3 MA. FIG. 7 demonstrates summary on values of RE plateaus and inferred RE current fractions generated for all plasma disruption scenarios, including MGI/SPI experiments in JET-ILW in all range of disrupted current values. Increasing trend in generation of maximal RE current has been found with the increase of disrupted plasma currents and higher plasma current time derivative (FIG. 8) for all disruption scenarios. Revisiting previous results of [1,2,8,30], it was found that runaway

generation has been detected in JET-OPS scenarios at very low boundary safety factor q_{cyl} ≈ 2, and in JET-C and JET-ILW at $2.5 \le q_{95}(EFIT) \le 3$ highlighting obvious increasing trend in RE current values toward lower q (FIG.9) and FIG.10).





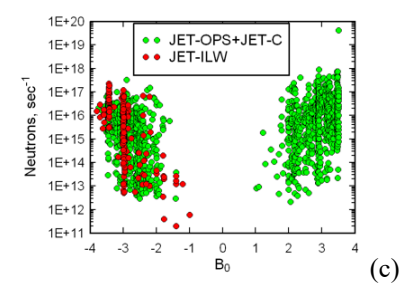


FIG.13 Role of toroidal magnetic field values and \vec{B}_0 direction on RE generation RE current values measured during spontaneous disruptions, those triggered by slow GIM puff and MGI+SPI and plotted as maximal I_{RE} fraction Optimization of MGI-SPI JET RE experiments obviously demonstrated absence of the "2T-threshold" on magnetic field for RE generation.

Data on RE obtained in JET-OPS experiments does not demonstrate detection of stable beams below toroidal magnetic field values $B_0 \le 1.8$ T and at positive direction of the vector \vec{B}_0 and (FIG. 11a). This result has been interpreted as extended loss of generated REs due to intense MHD activity during CQ which significantly degraded the RE confinement. Theoretical studies and numerical simulation of this data suggested that existing of such threshold is attributed to excitation of whistler instability [33].

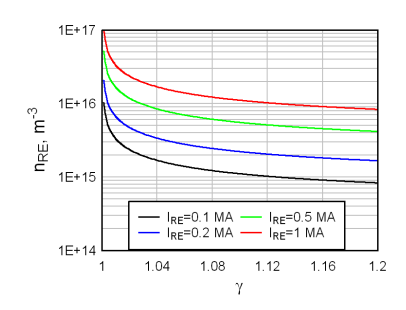
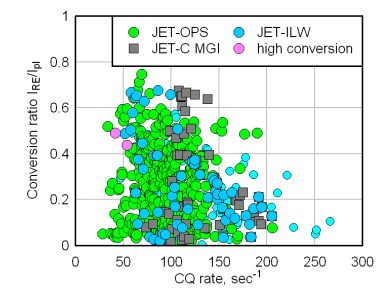


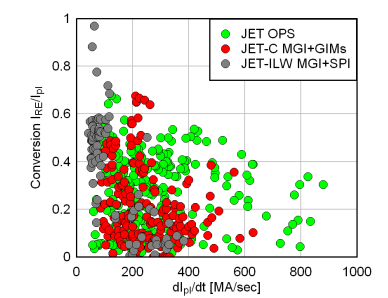
FIG. 14 Assessment of RE density in runaway beams with different currents depending on estimated runaway critical energies. RE density has been assessed from $N_e=2\pi R_0 I_{RE \ tot}/(ec\beta)$

After installation of ITER like Wall (JET-ILW) experiments on disruptions and REs have been carried out using MGI and SPI systems in L-mode target plasmas, in divertor and limiter configurations in a wide range of JET-ILW parameters. Typical parameters immediately preceding the MGI (with different gas injections) or SPI used to trigger the disruptions were: electron density 1.E19 \leq n_e \leq 4.5E19 m⁻³, magnetic fields 1. T \leq B₀ \leq 3. T plasma current variation between 1.0 MA and 3.0 MA and central electron temperature $T_e \sim 1.5 \div 3$ keV. The highest value of RE current ($I_{RE} \approx 1.7$ MA) has been detected during 3.0 MA disruption at 3.45 T in elongated limiter plasma with DMV3 at 1.1 bar of argon and DMV2 at 12 bar of deuterium. Optimization of disruption scenario with MGI in JET-ILW allowed the generation of REs in surprisingly low magnetic fields 1 T \leq B₀ \leq 1.1 T with negative direction of \vec{B}_0 (FIG. 11b). A detailed scan of the photo-neutron emission intensity vs. toroidal magnetic field for both directions of \vec{B}_0 showed almost symmetrical photo-neutron radiation data for both direction

of \vec{B}_0 (FIG.11c). Therefore, unlike previous conclusions, a systematic analysis of the data on RE in JET-C and JET-ILW revealed an absence of the "so-called" threshold on magnetic field values. Top boundary of RE generation dependency on magnetic field values could be represented by function $\sim B_0^2$. Observed dependence apparently signifies about general effect of confinement on generated REs.

Important parameter for study of RE generation process is RE density evaluated from measured or deduced runaway current fractions. In particular, assessment of RE density values provided necessary data on evaluation of RE distribution function. Fig 14 presents data on RE density evaluated from given values of RE currents for different values of critical energy of runaway process (represented by Lorentz parameter γ_0): $I_{RE} = \frac{ec}{\gamma_0} \sqrt{\gamma_0^2 - 1} \frac{N_{RE}}{2\pi R_0}$. Here, N_{RE} is a total number of REs in plasma volume, I_{RE} is evaluated runaway current fraction, R₀ is major plasma radius. Calculations have been carried out for runaway beam currents: $I_{RE} = 0.1, 0.2, 0.5$ and 1 MA respectively. The assessed values of RE density in experiments are very close to those calculated with conventional equations for simulation of runaway process [8]. Parameters of REs were calculated taking into account results of study of plasma ion charge depending on Te [34] in frames of known models for runaways, which consist of the primary generation mechanism [5,6] and secondary avalanching [16,17]. Obtained parameters (RE density, current and assessment of energy) have been compared to those measured in experiments.





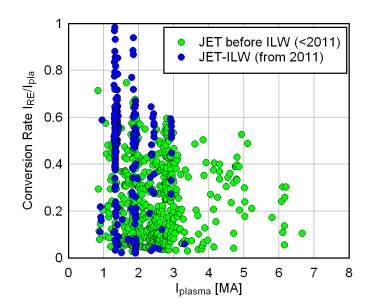


FIG.15 Decaying trend in disruption scenarios

the FIG.16 Decreasing trend in conversion FIG.17 Decreasing trend in conversion found for all JET operation stages.

dependence of current conversion ratio dependence vs. time derivative of ratio dependence on disrupted plasma I_{RE}/I_{pl} vs. CQ rates plotted for all JET disrupted plasma currents has been currents has been found for all JET operation stages.

A study of relationship between CQ parameters and RE generation dynamics constitutes one of the important tasks in analysis of the JET RE data-base. From the viewpoint of safety operations, fast plasma current decay during disruptions induces eddy currents which might cause severe damage to the vacuum vessel. As well, increase of plasma current time derivative and plasma currents can cause a severe increase of high energy RE populations. Analysis of JET data-base has examined plasma parameters during current decay and suggests several contra-expected results. First of all, unlike the results of [7, 8], FIG. 8 demonstrate that values of generated RE currents almost linearly increased with grow of disrupted plasma currents up to 3 MA. When disrupted currents exceed the threshold ≈3 MA the RE generation efficiency is falling. It might occur due to significant slowdown in the growth of RE populations with increase of plasma current time derivative (FIG.9) and also due decrease of CQ rate (FIG.10). However, FIG.11 shows controversial results, which could be conflicting with previous interpretations, since generated RE populations are diminishing with CQ rate increase (FIG.15). Also, in this FIG.

one can see apparent threshold in CQ rates values for runaway regime. In terms of conversion ratio of plasma currents into runaway currents (I_{RE}/I_{pl}) one can see in FIG.16 the decreasing trend in I_{RE}/I_{pl} vs. plasma current time derivative. Fig 17 demonstrates evolution of current conversion ratio I_{RE}/I_{pl} vs. plasma currents. FIG.17 highlights very clear decreasing trend in current conversion ratio evolution, I_{RE}/I_{pl} significantly falls for all disruption scenarios in whole range of disrupted plasma currents ($I_{pl} \le 7$ MA). The initial analysis of the observed phenomena draws attention to the relationship between RE energy evolution and RE currents and density dynamics. All presented RE characteristics will be examined in nearest future using numerical simulations of RE generation process having input parameters from the RE data-base.

4. SUMMARY

Experiments in JET provided large amount of data on disruptions and RE generation parameter dynamics allowing their extrapolation to scale of the ITER operation parameters. Collected data on RE generation events (>2000 in total) in JET disruptions covers all stages of JET operations. Runaways have been generated during spontaneous or deliberate disruptions in different plasma configurations: circular or elongated, limiter or divertor, etc. Extended analysis of RE database established key dependencies of main post-disruption RE parameters, such as, RE densities, currents and current conversion ratios (I_{RE}/I_{pl}) on pre-disruption plasma currents, plasma current time derivatives, CQ rates, safety factor $q_{95}/q(a)$, pre-disruption density, temperature, etc. In several experiments with MGI and SPI the HXR/ γ and photo-neutrons diagnostics measured maximal energies of runaways $E_{MAX} \leq 10 \div 12$ MeV. Analysis of SPI experimental results and data from experiments with MGI using different DMVs revealed different influence on disruption dynamics and RE generation. One of the important results from the data-base analysis is observation of clear threshold in RE generation on CQ rates. A decreasing trend in conversion ratio I_{RE}/I_{pl} has been established vs. main parameters, such as pre-disruption plasma currents, plasma current time derivatives and CQ rates. Presented data-base on RE in JET requires further extended study including analysis of the disruption phenomenology and numerical simulations of runaway generation dynamics.

ACKNOWLEDGEMENTS

This work has been carried out within the framework of the EUROfusion Consortium, funded by the European Union via the Euratom Research and Training Programme (Grant Agreement No 101052200 — EUROfusion). Views and opinions expressed are however those of the author(s) only and do not necessarily reflect those of the European Union or the European Commission. Neither the European Union nor the European Commission can be held responsible for them. The views and opinions expressed herein do not necessarily reflect those of the ITER Organization. IPFN activities were supported by FCT – Fundação para a Ciência e Tecnologia, I.P., under project references UID/50010/2023, UID/PRR/50010/2025, and LA/P/0061/2020.

REFERENCES

- [1] ITER Physics Basis, 1999 Nuclear Fusion (39) 2137.
- [2] T.C. Hender et al 2007 Nuclear. Fusion 47 S128-202. Progress in the ITER Physics Basis.
- [3] A. Loarte et al. 2025 Plasma Phys. Control. Fusion 67 065023, The new ITER baseline, research plan and open R&D issues
- [4] J. Wesson, R. D. Gill, M. Hugon et al. 1989 Nuclear Fusion 29 641 Disruptions in JET
- [5] H. Dreicer 1959 Phys. Rev. 115 238–249; Dreicer H. 1960 Phys. Rev. 117 329–342. I and II.
- [6] H. Knoepfel, D.A. Spong 1979 Nuclear Fusion 19 785 Runaway electrons in toroidal discharges.
- [7] R. D. Gill et al. 2002 Nuclear Fusion 42 1039 Behavior of disruption generated runaways in JET
- [8] V. V. Plyusnin et al. 2006 Nuclear Fusion 46 277 Study of runaway electron generation during major disruptions in JET
- [9] C. Reux et al 2015 Nuclear Fusion 55/129501;
- [10] Y. Kawano et al. 2005 Journal of Plasma and Fusion Research V.81, No.8;
- [11] R.J. Zhou et al. 2017 Nuclear Fusion 57 114002.
- [12] C. Reux et al. 2010 Nuclear Fusion 50 095006
- [13] Hollmann E M et al 2013 Nuclear Fusion 53 083004
- [14] V.V. Plyusnin et al 2018 Nuclear Fusion 58 016014
- [15] L.-G. Eriksson et al. 2004 Phys. Rev. Letters, V.92 p. 205004
- [16] Yu. A. Sokolov. 1979 JETP Letters 29, 218, "Multiplication" of accelerated electrons in a tokamak.
- [17] M. N. Rosenbluth and S. V. Putvinski 1997 Nuclear Fusion 37, 1355
- [18] Nygren R. et al 1997 Journal of Nuclear Materials 241 3, 522
- [19] E. Hollmann E et al 2015 Phys. Plasmas 22 021802 Status of research toward the ITER disruption mitigation system.
- [20] M. Lehnen et al 2011 Nuclear Fusion 51 123010
- [21] M. Lehnen et al. R&D for reliable disruption mitigation in ITER. 2018 IAEA Fusion Energy Conf. (Gandhinagar, India, 22-27 October)
- [22] Baylor L R et al. 2019 Nuclear Fusion 59 066008.
- [23] D. Shiraki et al 2018 Nuclear Fusion 58 056006.
- [24] Reux C et al. 2021 Phys. Rev. Lett. 126 175001.
- [25] S. Giors et al. 2025 Fusion Engineering and Design, V. 216, July 2025, 115116
- [26] S. Jachmich et al 2022 Nucear Fusion 62 026012. Shattered pellet injection experiments at JET in support of the ITER disruption...
- [27] N. A. Garland et al. 2020 Phys. Plasmas 27 040702.
- [28] Harris G.R.1990 Preprint JET-R(90)07
- [29] Jarvis O.N. et al. 1988 Nuclear Fusion 28 1981;
- [30] V.G. Kiptily et al. 2006 Plasma Phys. Control. Fusion 48 R59
- [31] P. H. Rebut et al., 1985 Nuclear Fusion 25, 1011
- [32] A. Shevelev et al, 2013 Nuclear Fusion 53/123004
- [33] Fülöp T., Smith H.M. and Pokol G. 2009 Phys. Plasmas 16 022502
- [34] D. Kh. Morozov, E. O. Baronova, I. Yu. Senichenkov. 2007 Plasma Physics Reports, V33, No 11, p.906